

# Theory and experiment of the ESR of $\text{Co}^{2+}$ in $\text{Zn}_2(\text{OH})\text{PO}_4$ and $\text{Mg}_2(\text{OH})\text{AsO}_4$

M.E. Foglio, M.C dos Santos and G.E. Barberis  
*Instituto de Física "Gleb Wataghin", UNICAMP,  
13083-970, Campinas, São Paulo, Brazil.*

J.M. Rojo, J.L. Mesa, L. Lezama and T. Rojo  
*Departamento de Química Inorgánica. Universidad del País  
Vasco.  
48080 Bilbao, Spain  
(October 24, 2018)*

## Abstract

Experiments of Electron Spin Resonance (ESR) were performed on  $\text{Co}^{2+}$  substituting  $\text{Zn}^{2+}$  or  $\text{Mg}^{2+}$  in powder samples of  $\text{Zn}_2(\text{OH})\text{PO}_4$  and  $\text{Mg}_2(\text{OH})\text{AsO}_4$ . These two compounds are iso-structural and contain the  $\text{Co}^{2+}$  in two environments of approximately octahedral and trigonal bipyramidal structures. The observed resonances are described with a theoretical model that considers the departures from the two perfect structures. It is shown that the resonance in the penta-coordinated complex is allowed, and the crystal fields that would describe the resonance of the  $\text{Co}^{2+}$  in the two environments are calculated. The small intensity of the resonance in the penta-coordinated complex is explained assuming that this site is much less populated than the octahedral one; this assumption was verified by a molecular calculation of the energies of the two environments, with both Co and Zn as central ions in  $\text{Zn}_2(\text{OH})\text{PO}_4$ .

76.30.Fc,71.70.Ch,31.15.-p,31.15.Ct

## I. INTRODUCTION

Mineral solid state chemistry offers an important contribution to materials science [1] in the search for systems with new and useful physical properties. The phosphate and arsenate minerals crystallize in various structures, sometimes containing several non-equivalent sites for the metals. The minerals of the olivine group, with the  $ABXO_4$  formula, have been known for a long time [2], and the adamite family, with formula  $[M_2(O/OH)(XO_4)]$ , belongs to this group and takes its name from the natural compound [3,4]  $Zn_2(OH)AsO_4$ . The compounds studied in this work belong to this family, and the cations can occupy two sites with rather different environments, one being octahedral and the other penta-coordinated, so that rather different magnetic properties could be expected when magnetic cations are employed. The recently synthesized compounds  $Zn_2(OH)PO_4$  [5],  $Co_2(OH)PO_4$  [5],  $Mg_2(OH)AsO_4$  [6,7], as well as the natural  $Co_2(OH)AsO_4$  [1], are of the adamite type and present these two type of sites. We have then found interesting to study the properties of the  $Co^{2+}$  ions as impurities in the two non-magnetic compounds, as a first step in the understanding of the properties of the concentrated compounds.

Electron Spin Resonance (ESR) is a fruitful technique to obtain local information of the environment of the magnetic ion, and the  $Co^{2+}$  ion is particularly useful for this kind of study because its  $g$  value has a strong crystal field dependence in these compounds. To analyze the ESR measurements it is necessary to have information about the splitting of the energy levels with both the crystal field and the electronic Coulomb repulsion, and to obtain this information we employed optical diffuse reflectance measurements [8].

The experimental ESR powder spectra of  $Co^{2+}$  impurities in both  $Zn_2(OH)PO_4$  and  $Mg_2(OH)AsO_4$  present two different sets of lines, one very intense, and the other just observable. The average of the  $g$  factors of the intense spectra is 4.15 in the two compounds, a value close to the 4.33 expected for  $Co^{2+}$  in moderately distorted octahedral symmetry [9], and it seems reasonable to assign these spectra to that environment and apply the approach already employed [10] in the study of the ESR of  $Co^{2+}$  in  $NH_4NiPO_4 \cdot 6H_2O$ , where the crystal fields that reproduce the observed spectra were obtained. As the remaining lines are very weak one should analyze whether they belong to the penta-coordinated symmetry, and in that case the possible reason for their small intensity.

We are not aware of any theory describing the ESR of  $Co^{2+}$  in the penta-coordinated environment, a distorted trigonal bipyramid, and we first calculated the crystal fields of the perfect trigonal bipyramid following the existing literature [11,12]. To analyze the distorted complex we derived the normal modes of the trigonal bipyramid with respect to the reference complex, and then obtained the Jahn-Teller contributions [13,14] to the crystal field acting on the  $Co^{2+}$ , that is generated by these modes.

In this calculation we have introduced a procedure that uniquely defines the orientation and size of the two reference complexes, so that the normal modes that describe their deformation are free from irrelevant rotations and expansions.

These results were then employed to calculate the theoretical ESR spectra. We found that for the system parameters obtained from the optical spectra we should expect that the ground doublet be  $M_J = \pm 1/2$ , corresponding to an allowed spectrum. The rather small intensity, of this type of spectra seems to indicate a preference of  $Co^{2+}$  for the octahedral sites in the crystal structure, a conjecture that was advanced in a preliminary report [15]

on the ESR of impurities of this ion in  $\text{Mg}_2(\text{OH})\text{AsO}_4$ , and that is confirmed in the present work. Employing a molecular calculation we have also verified that the formation energies of the two type of complexes, with both Co and Zn as the central ions, are compatible with this hypothesis.

The description of the experiments, and experimental analysis of the data is presented in Section II. The theory of the ESR of the  $\text{Co}^{2+}$  in a distorted trigonal bipyramid is presented in Section III, together with the theoretical analysis of the two type of complexes in the two compounds. A discussion of our results is presented in Section IV together with our conclusions.

## II. EXPERIMENTAL

### A. Synthesis and characterization of the materials.

Compounds with  $\text{Co}^{2+}$  substituting Mg and Zn in  $\text{Zn}_2(\text{OH})\text{PO}_4$  and  $\text{Mg}_2(\text{OH})\text{AsO}_4$  were prepared by hydrothermal synthesis, starting from the  $(\text{M}, \text{Co})_3(\text{XO}_4) : 8\text{H}_2\text{O}$  ( $\text{M} = \text{Zn}, \text{Mg}$ ) vivianites, previously prepared as reported elsewhere [16]. Approximately 0.200 g. of these precursors were disaggregated in *ca.* 75 mil. of water and were placed in a poly(tetrafluoroethylene)-lined stainless steel container (about three quarters full) under autogenous pressure. The reaction was carried out at  $180^\circ \text{C}$  and maintained for one week. The resulting microcrystalline products were filtered off and washed with ether and dried in air.

The results of the analysis of Mg, Zn, Co, P, and As by inductively coupled plasma atomic emission spectroscopy (ICP-AES) are in good agreement with the proposed formulae. The compounds were also characterized by X-ray powder diffraction, using the Rietveld method. The diffractograms were indexed with the  $P_{nmm}$  space group and the lattice parameters  $a = 8.042(3) \text{ \AA}$ ,  $b = 8.369(2) \text{ \AA}$  and  $c = 5.940(2) \text{ \AA}$  for the phosphate compound and  $a = 8.286(2) \text{ \AA}$ ,  $b = 8.594(2) \text{ \AA}$  and  $c = 6.051(1) \text{ \AA}$  for the arsenate. The parameters of the phosphate compound are only slightly different from those given in reference [5], while those of the arsenate coincide with the data published by other authors [6,7]; the results obtained in the last three references were performed in single crystals. The X-ray powder pattern was recorded employing Cu Ka radiation with a PHILIPS X'PERT automatic diffractometer, with steps of  $0.02^\circ$  in  $2\Theta$  and fixed-time counting of 1 s in the  $5 < 2\Theta < 70^\circ$  range. We preferred to use our own experimental parameters in the present paper.

### B. Optical studies.

The necessary optical data were obtained from diffuse reflectance experiments, performed in a CARY 2415 UV-VIS-IR spectrometer, controlled with a VARIAN DS15 workstation, in the  $5000 - 50000 \text{ cm}^{-1}$  wavenumber region [8,17]. The whole of the optical data used in this work was recorded at room temperatures, and all the relevant data that was necessary in the present work is in the tables I and II. Figure 1 presents the experimental data for both the phosphate and the arsenate Co compounds studied in this paper. The system parameters of the octahedral complexes are slightly different from those already published [8,17], because

they were obtained from the optical spectra after including a spin orbit correction in the ground orbital level [18].

### C. Electron Spin Resonance (ESR).

The ESR spectra were performed at X Band on a Bruker ESP300 spectrometer. Cooling and temperature control of the samples were obtained with a standard OXFORD helium continuous-flow cryostat, included in the microwave cavity. Magnetic field measurements were done simultaneously with the ESR spectra recording, using a Bruker ER035M NMR gaussmeter. The resonant frequency of the cavity was measured with a Hewlett-Packard 5352B microwave frequency counter.

Only powder spectra could be measured for the two systems studied here because it was not possible to obtain single crystals, and small concentrations of Co (1% in the arsenate and 0.1% in the phosphate) substitute the metals in the two lattices. The curves denoted with (a) in Figs. 2 and 3 show the measured ESR spectra for the two samples, recorded at 4.2 K, and they both clearly show three sets of lines with a well defined hyperfine structure that identifies the  $\text{Co}^{2+}$  ion. There are also some extra lines, rather weak in the phosphate but more intense in the arsenate, that preclude an automatic fitting of the spectra. We have then simulated the powder spectra of the hexa-coordinated  $\text{Co}^{2+}$  with a program which allows any symmetry, line positions, hyperfine tensor, and linewidth anisotropies, and our best results, plotted in the curves (c) of Figs. 2 and 3, correspond to the  $g$ -values shown in rows a) of table III Their values and positions are also shown by arrows below the simulated curves (c).

The extra lines near 200 mT in the phosphate show an hyperfine structure typical of the  $\text{Co}^{2+}$ , and are given in more detail in the inset of Fig. 2. The remaining lines in the two compounds are rather broad and show a collapsed hyperfine structure. The curves (b) in the Figs. 2 and 3 show the sum of the simulated spectra of the hexa-coordinated  $\text{Co}^{2+}$  in (c), plus a simulation of the penta-coordinated  $\text{Co}^{2+}$  that employs the  $g$ - values given in rows b) of table III and is adequately renormalized to account for the smaller relative concentration of the last compound. These  $g$  values have rather large errors, and their positions are shown by arrows above the measured spectra (a) of Figs. 2 and 3. In the inset of Fig. 2 it is also shown the detail of the hyperfine structure near 200 mT both in the experimental and in the simulated spectrum.

The assignment of the extra lines to the penta-coordinated complex shall be further discussed in section III B 5.

## III. THEORETICAL DISCUSSION

### A. Hexa-coordinated Co

We shall first discuss the hexa-coordinated  $\text{Co}^{2+}$  ions, that are surrounded by six oxygens in a fairly regular octahedron with positions given in table IV. In the present case we have a powder spectra, and we could only measure the three principal values  $g_i$  of the  $\mathbf{g}$  tensor (see table III). As in a previous work [10] we shall consider the effect that the crystal field

generated by the normal modes of the octahedron has on the gyromagnetic tensor  $\mathbf{g}$ . This method systematizes the procedure, and in table V we give the normal modes that reproduce the experimental values of the three  $g_i$ . We shall then choose a reference perfect octahedron centered in the  $\text{Co}^{2+}$ , calculate the normal modes corresponding to the crystallographic positions of the O, and compare them in table V with those obtained from the experimental spectra.

Only the normal coordinates that are invariant against inversion with respect to the center of the octahedron are necessary in the present problem, [19,10] and these are separated into the three sets  $\{Q_1\}$ ,  $\{Q_2, Q_3\}$  and  $\{Q_4, Q_5, Q_6\}$ , with the corresponding  $Q_j$  transforming respectively like the basis of the irreducible representations  $A_1$ ,  $E$  and  $T_2$  of the cubic group, as given in table II of reference [20].

The  ${}^4F$  ground state of isolated  $\text{Co}^{2+}$  ( $3d^7$ ) in a purely octahedral crystal field splits into two orbital triplets  ${}^4T_1, {}^4T_2$  and one orbital singlet  ${}^4A_2$ . Spin-orbit effects partially lift the degeneracy of the  ${}^4T_1$  triplet into one  $\Gamma_6$ , two  $\Gamma_8$  and one  $\Gamma_7$  subspaces, and the resonance for the lowest doublet ( $\Gamma_6$ ) is isotropic with  $g = 4.33$  [9]. The addition of lower symmetry crystal fields produce further splitting of the  ${}^4T_1$  triplet, giving six Kramer's doublets, and in most cases it is found that the trace of the  $g$  tensor is close to the cubic isotropic value; [21] in the present case the average  $g$  is 4.1537 for  $\text{Co}:\text{Zn}_2(\text{OH})\text{PO}_4$  and 4.153 for  $\text{Co}:\text{Mg}_2(\text{OH})\text{AsO}_4$ . To understand these values it is sufficient to consider the  $\text{Co}^{2+}$  in pure octahedral symmetry, because the crystal fields of lower symmetry do not change this value in our approximation. The calculation follows the same lines given in reference [10] and shall not be repeated here.

In the lowest order one obtains  $\mathbf{g}$  from the matrix elements of the Zeeman term in the  $\Gamma_6$  subspace of the  ${}^4T_1$  ground triplet. The matrix elements of the orbital angular momentum  $\mathbf{L}$  within a  $T_1$  subspace are proportional to those of a  $P$  term, but one should note that the excited term  ${}^4P$  is also of the  ${}^4T_1$  symmetry, and is mixed by the cubic field with the  ${}^4T_1$  of the ground  ${}^4F$  term. If we indicate two states of  ${}^4F$  and  ${}^4P$  with  $\phi_i$  and  $\phi'_i$  respectively, such that they transform in the same way under the cubic group, the states of the ground  ${}^4T_1$  will be of the form  $a\phi_i + b\phi'_i$ . The values of the constants  $a$  and  $b$  can be obtained [22,23] from the Racah parameter  $B$  and the crystal field parameter  $D_q$ , that were estimated [18] from the spectroscopic data and are given in table I. With these values one obtains  $a = -0.9820$  and  $b = 0.1886$  for the phosphate, and the proportionality constant of the angular momentum is then

$$\alpha = -1.5 a^2 + b^2 = -1.4110. \quad (1)$$

To analyze further the experimental  $\mathbf{g}$  tensor, one could try and find crystal field values that would reproduce the measured results, and a study of this type was presented by Abragam and Pryce for the Cobalt Tutton salts. [24] To simplify the study we present a model that describes all the crystal fields acting on the Co as originating in the crystal field of the six nearest O located at the vertices of a deformed octahedron, obtained by displacement of the vertices of the reference octahedron. If one neglects the mixing of other configurations into the ground configuration  $(3d)^7$ , it is sufficient to keep only the part of the crystal field  $V$  that is even against inversion. We could then write  $V = \sum_{i=1}^7 V(\mathbf{r}_i)$ , where  $V(\mathbf{r})$  would be the sum of homogeneous polynomials of second and fourth order in the components  $x, y, z$  of the electronic coordinates  $\mathbf{r}$ . Within our model, one could then write [19]

$$V(\mathbf{r}) = \sum_j Q_j V_j(\mathbf{r}) \quad (2)$$

where the  $Q_j$  and  $V_j(\mathbf{r})$  transform like the same partners of irreducible representations of the octahedral group [20]. As the  $V_j(\mathbf{r})$  must be even against inversion, the  $Q_j$  must have the same property, and only the six  $Q_j$  with  $j = 1, 6$  discussed at the beginning of this section would appear in Eq. (2), but we shall not consider the identical representation  $A_1$  because it does not modify the  $g$  tensor. The useful  $V_j(\mathbf{r})$  are given in Eqs. (4-6) from reference [10].

To study the effect that the  $V(\mathbf{r})$  given in Eq.(2) has on the  $g$  tensor of, we shall employ second order perturbation theory [25], using both  $V(\mathbf{r})$  and the Zeeman term  $H_Z = (g_e \mathbf{S} + \mathbf{L}) \cdot \mathbf{H}$  as perturbation. The change  $\delta \mathbf{g}$  in the  $g$  tensor is then obtained from

$$\begin{aligned} \mathbf{S} \cdot \delta \mathbf{g} \cdot \mathbf{H} = & \frac{2}{3} (g_e + \alpha) \frac{\mu_B}{\Delta} \left\{ -C_E \left[ \sqrt{3} Q_2 (S_x H_x - S_y H_y) + \right. \right. \\ & Q_3 (3S_z H_z - \mathbf{S} \cdot \mathbf{H}) \left. \right] + C_T \left[ Q_4 (S_z H_y + S_y H_z) + \right. \\ & \left. \left. Q_5 (S_x H_z + S_z H_x) + Q_6 (S_x H_y + S_y H_x) \right] \right\}, \quad (3) \end{aligned}$$

where  $\mu_B$  is the Bohr magneton,  $\Delta$  is the splitting between the  $\Gamma_6$  doublet and the lowest  $\Gamma_8$  quadruplet in the octahedral symmetry, and  $\Delta = 283 \text{ cm}^{-1}$  in the P compound.

The values of  $C_E$  and  $C_T$  are obtained by the same procedure employed in reference [10], obtaining  $\langle r^4 \rangle$  from the cubic field parameter  $D_q$  and  $\langle r^2 \rangle$  from the ratio  $\langle r^2 \rangle / \sqrt{\langle r^4 \rangle} = 0.6544$  of the calculated values [23]. For the Co-O distance  $R$  we used  $R = 2.11176 \text{ \AA}$ , corresponding to the reference octahedron defined below, and we found the values  $C_E = 6436 \text{ cm}^{-1}/\text{\AA}$  and  $C_T = -3666 \text{ cm}^{-1}/\text{\AA}$ . We can now calculate the crystal fields that would describe the experimental values of  $\mathbf{g}$  or, what is equivalent, the corresponding normal modes within the approximations just discussed. As there are more normal modes than data, we fix the relations  $Q_4 = Q_3 = 0.3044 Q_6$ , which correspond to the normal modes calculated below from the crystallographic positions, and we obtain a perfect fit to the experimental values employing the normal modes given table V.

From table I we obtain the coefficients  $a = -0.9824$ ,  $b = 0.1867$ , and  $\alpha = -1.4128$  for  $\text{Co}_2(\text{OH})\text{AsO}_4$ . The ESR data was then adjusted with the normal modes coordinates given in table V, where we used  $R = 2.1224 \text{ \AA}$ ,  $Q_4 = Q_3 = 0.4037 Q_6$ ,  $C_E = 6287 \text{ cm}^{-1}/\text{\AA}$ ,  $C_T = -3558 \text{ cm}^{-1}/\text{\AA}$  and  $\Delta = 282 \text{ cm}^{-1}$ , for this compound.

To calculate the crystallographic normal modes of the octahedron it is necessary to chose a reference perfect octahedron centered in the  $\text{Co}^{2+}$ . To this purpose we consider the three normal modes of pure rotation, [19]  $Q_{19}$ ,  $Q_{20}$ , and  $Q_{21}$ , and we chose the axes of the reference octahedron so that these three normal coordinates are zero, because they should not have any effect on the properties of the complex. The value  $R = 2.11176 \text{ \AA}$  of the Co-O distance in the reference octahedron was chosen so that  $Q_1 = 0$ , and by this whole procedure we obtain a unique reference octahedron and minimize the effect of irrelevant rotations and expansions on the values of the normal modes. The direction cosines of the three Co-O directions in the reference octahedron are given in table VI, and the normal modes derived from the crystallographic ionic positions given in table IV are shown in the third line of table V. The normal modes calculated from the crystallographic position of the O in the octahedral complex are different than those obtained from the experimental  $\mathbf{g}$  tensor, given in the first line of the same table. This result indicates that although the nearest O to the Co

are the main source of the cubic field, [19] the remaining non-cubic perturbations have strong contributions due to the rest of the crystal. We conclude that the experimental  $\mathbf{g}$  tensor could be explained by the crystal field  $V(\mathbf{r})$  of Eq. (2) given in the axes of the reference octahedron defined in table VI with the  $Q_j$  given in the row a) of table V. The agreement is perfect because there are more free normal coordinates than available  $\delta\mathbf{g}$  components, but the theory presented can only be considered a first approximation. In particular, although the crystal field theory of point charges gives the right symmetry properties, it is only a very rough description of the physics of the problem.

Although we have not analyzed the hyperfine tensor in detail, we have verified that its components are compatible with the normal modes necessary to describe the  $\delta\mathbf{g}$  tensor.

In the present calculation we have neglected the effect of the  ${}^4T_2$  triplet, that contributes to  $\delta\mathbf{g}$  in third order perturbation (our calculation would be of the second order). This effect was calculated by Tucker [23] who obtained contributions that are about 6% of the second order contribution for the  $T_2$  deformation and about 13% for the  $E$  deformation, and would therefore not alter substantially our conclusions.

## B. Penta-coordinated Co

### 1. The crystal field of the trigonal bipyramid.

The structure of the penta-coordinated complex of  $\text{Co}^{2+}$  is very close to a trigonal bipyramid, and the positions of the Co and of the five O are given with respect to the crystal axes in table VII. Following a method similar to that employed in the octahedral case we chose an orthogonal system of axes X,Y,Z, such that the normal modes obtained from the crystallographic positions would not have contributions of irrelevant rotations and expansions. The direction cosines of the axes of this system with respect to the crystal axes  $\mathbf{a}$ ,  $\mathbf{b}$  and  $\mathbf{c}$  are given in table VIII, and the coordinates of the six atoms in the reference perfect trigonal bipyramid are given in table IX. There are two different Co-O distances in the reference complex:  $R_a$  corresponds to the three ligands in the XY plane (equatorial O) and  $R_c$  to the two along the Z axis (axial O); their values for the phosphate and arsenate are given in the caption of table IX. Two crystal field parameters  $D_s$  and  $D_t$  are necessary in the trigonal bipyramid, and are given in the point charge model by: [11,26]

$$\begin{aligned} D_s &= \frac{e}{14} \left[ \frac{4q_c}{R_c^3} - \frac{3q_a}{R_a^3} \right] \langle r^2 \rangle, \\ D_t &= \frac{e}{168} \left[ \frac{16q_c}{R_c^5} + \frac{9q_a}{R_a^5} \right] \langle r^4 \rangle, \end{aligned} \quad (4)$$

where we shall use  $q_a = q_c = -2e$ . The crystal field potential  $V_{cf}$  can be expressed by the usual formula

$$V_{cf}(\mathbf{r}) = \sum_{kq} \sqrt{\frac{4\pi}{2k+1}} \sum_{\ell} q_{\ell} \frac{r_{\ell}^k}{r_{\ell}^{k+1}} Y_{kq}^*(\theta_{\ell}, \varphi_{\ell}) C_q^{(k)}(\theta, \varphi), \quad (5)$$

where  $Y_{kq}(\theta_{\ell}, \varphi_{\ell})$  are the spherical harmonics at the position of the  $\ell$ -th ligand and the  $C_q^{(k)}(\theta, \varphi) = \sqrt{4\pi/(2k+1)} Y_{kq}(\theta, \varphi)$  are usually called the Racah's rationalized spherical

harmonics. In our actual calculation we have employed the real combinations  $C_{lm}(\theta, \varphi)$  and  $S_{lm}(\theta, \varphi)$  that are proportional to  $\cos(m, \varphi)$  and  $\sin(m, \varphi)$  respectively [27]. In the absence of the spin-orbit interactions one employs the irreducible representations  $\Gamma$  of the trigonal bipyramid to classify the eigenstates  $|\alpha, S, L, \Gamma, \gamma, a\rangle$  of the Hamiltonian, which are simply related to the states  $|\alpha, S, L, M_L\rangle$  (the index  $\alpha$  identifies the particular states with the same  $S, L$ ). In table I of reference [11] we find that the irreducible representations  $A'_2, A''_1, A''_2, E'$  and  $E''$  are contained in the two terms  ${}^4F$  and  ${}^4P$ , and that the  $|\alpha, S, L, M_L\rangle$  states that generate the corresponding subspaces are  $\{|3, 3/2, 3, 0\rangle, |3, 3/2, 1, 0\rangle\} \rightarrow A'_2$ ,  $\{|3, 3/2, 3, \pm 3\rangle\} \rightarrow (A''_1, A''_2)$ ,  $\{|3, 3/2, 3, \pm 2\rangle\} \rightarrow E'$  and  $\{|3, 3/2, 3, \pm 1\rangle, |3, 3/2, 1, \pm 1\rangle\} \rightarrow E''$ . The Hamiltonian without spin orbit interaction is diagonal in the partners  $\gamma$  of each irreducible representation  $\Gamma$  and in the spin component  $M_S$ , so it is not necessary to write them explicitly here. The only  $C_q^{(k)}(\theta, \varphi)$  that contribute to Eq.(5) in the perfect trigonal bipyramid have  $k = 0, 2, 4$  and  $q = 0$ . To calculate the matrix elements of the Hamiltonian that contains  $V_{CF} = \sum_{i=1,7} V_{cf}(\mathbf{r}_i)$ , we have used the standard tensorial operator techniques [28] as well as the unitary operators obtained from Nielsen and Koster's tables [28,29], and we have verified that our matrix coincides with that given in table II or reference [11].

Our main objective here is to find the gyromagnetic factors that one would expect to measure in the penta-coordinated  $\text{Co}^{2+}$ , and we shall employ the spectroscopic data measured by diffuse reflectance to estimate the parameters  $B, D_s$  and  $D_t$  for both  $\text{Co}:\text{Zn}_2(\text{OH})\text{PO}_4$  and  $\text{Co}:\text{Mg}_2(\text{OH})\text{AsO}_4$ . In the two rows labeled a) of table II we give the corresponding assignments of the transitions from the ground  ${}^4A'_2$  to the levels with symmetry  ${}^4A''_1, {}^4A''_2, {}^4E'', {}^4E', {}^4A'_2(P)$  and  ${}^4E''(P)$ , where we use  $(P)$  to indicate the higher levels of the same symmetry.

From the eigenvalues of the Hamiltonian in the absence of the spin-orbit interaction, we find by trial and error the values of  $B, D_s$  and  $D_t$  that minimize the mean square deviation  $\chi$  for the two systems, and we give them in row b) of table X. The transitions calculated with these two sets of values are given in the two rows of table II that are labeled b). The fitting is rather poor, and in particular the transitions to the levels  ${}^4A''_1, {}^4A''_2$  and  ${}^4E''$  fall below the range of the measuring equipment. As an alternative we have fitted only the three highest transitions, obtaining the values given in row c) of table X, and the corresponding values calculated with these two sets of parameters are given in the two rows of table II that are labeled c). In the following section we shall consider these two sets of values to estimate the gyromagnetic factors for each of the two compounds.

## 2. The spin-orbit interaction in the trigonal bipyramid.

It is now essential to include the spin orbit interaction into the calculation. The basis of the irreducible representations  $\Gamma_7, \Gamma_8$  and  $\Gamma_9$ , of the double group  $D_{3h}^*$  have a simple expression in our system: [12] they are given by  $|d^7\alpha SLJM_J\rangle$ , and in particular we have  $\Gamma_7(a) \equiv \{|d^7\alpha SLJ \pm 1/2\rangle\}$ ,  $\Gamma_7(b) \equiv \{|d^7\alpha SLJ \pm 11/2\rangle\}$ ,  $\Gamma_8(a) \equiv \{|d^7\alpha SLJ \pm 5/2\rangle\}$ ,  $\Gamma_8(b) \equiv \{|d^7\alpha SLJ \pm 7/2\rangle\}$ ,  $\Gamma_9(a) \equiv \{|d^7\alpha SLJ \pm 3/2\rangle\}$  and  $\Gamma_9(b) \equiv \{|d^7\alpha SLJ \pm 9/2\rangle\}$ . These states are easily obtained from the  $|d^7, \alpha, S, M_S, L, M_L\rangle$  calculated above by employing the 3-j or the Clebsch Gordan coefficients. In the absence of magnetic fields the two states of each Kramer's doublet have the same energy, and to calculate the energies of the system it is enough to consider only the states with positive  $M_J$ . As only the mixture of

the  ${}^4F$  and  ${}^4P$  states is important in our problem we shall consider only that subspace, and the corresponding matrix of the total Hamiltonian splits into five boxes of the following dimensions:  $(M_J = 1/2) \rightarrow \Gamma_7(a) \rightarrow (7 \times 7)$ ,  $(M_J = 3/2) \rightarrow \Gamma_9(a) \rightarrow (6 \times 6)$ ,  $(M_J = 5/2) \rightarrow \Gamma_8(a) \rightarrow (4 \times 4)$ ,  $(M_J = 7/2) \rightarrow \Gamma_8(b) \rightarrow (2 \times 2)$ ,  $(M_J = 9/2) \rightarrow \Gamma_9(b) \rightarrow (1 \times 1)$ , and there are no matrix elements of  $M_J = 11/2$ , i.e.  $\Gamma_7(b)$ , within the subspace  $\{{}^4F, {}^4P\}$  of  $d^7$  that corresponds to  $S = 3/2$ . The matrices we have obtained coincide with those given in table II of reference [12], and their eigenvalues have been calculated for the different sets of  $B$ ,  $D_s$  and  $D_t$  values that were obtained above, employing the one-electron spin-orbit parameter  $\zeta = 580 \text{ cm}^{-1}$ . For all the set of parameters in table X the lowest doublet is a  $\Gamma_7(a)$  ( $M_J = \pm 1/2$ ), separated by at least  $75 \text{ cm}^{-1}$  from the following  $\Gamma_9(a)$  ( $M_J = 3/2$ ) doublet, and by more than  $2377 \text{ cm}^{-1}$  from the remaining doublets. This situation is not altered by making fairly large changes in the three basic parameters  $B$ ,  $D_s$  and  $D_t$ , and shows that even for moderate increases in the temperature only the lowest doublet ( $M_J = \pm 1/2$ ) would be occupied. This doublet has allowed ESR transitions, and should be observed within the approximation employed. If the position of the two lowest doublets were exchanged, the ESR transitions of the lowest doublet would be forbidden and the spectra should not be then observed.

The fact that the two lowest doublets have  $M_J = \pm 1/2$  and  $M_J = \pm 3/2$  and are separated by a large energy from the remaining doublets is easily understood when we notice that the lowest level in the absence of spin-orbit interaction is  ${}^4A'_2$ . The orbital part  $A'_2$  is a singlet with no orbital angular momentum, and the total  $\mathbf{J}$  would then correspond to the  $S = 3/2$ . These four states would be rather far apart from the remaining ones, and would split in the way calculated above through the higher order spin orbit mixing with those excited states.

The present calculation was for a perfect trigonal bipyramid with  $D_{3h}$  symmetry, and one wonders whether the deformations with respect to this structure could alter the relative position of the two lowest doublets, thus changing from an allowed to a forbidden ESR transition. We shall then study the effect of these deformations, both on the relative position of the two lowest doublets and on the value of the gyromagnetic tensor. In this study we shall follow a treatment similar to that employed in the octahedral case, by considering the effect of the normal modes of the trigonal bipyramid on the Hamiltonian of the penta-coordinated  $\text{Co}^{2+}$ .

### 3. The normal modes of the trigonal bipyramid

As in the octahedral case we are interested in a contribution to the Hamiltonian of the same type of Eq. (2), but here the normal modes  $Q_j$  and  $V_j(\mathbf{r})$  transform like the same partners of irreducible representations of the trigonal bipyramid. As the undistorted complex does not have a center of symmetry, both the even and odd modes against reflection in the equatorial plane may have non-zero matrix elements inside the configuration  $d^7$  of  $\text{Co}^{2+}$ , and therefore we shall need to consider both types of normal modes in our discussion.

The departures of the six atoms of the complex span a reducible representation  $\Gamma$  of the  $D_{3h}$  group, that can be reduced as follows:  $\Gamma = 2A'_1 + A'_2 + 4E' + 3A''_2 + 2E''$  (see e.g. the Eq. (9.19) in reference [30]). Of these irreducible representations, the  $A'_2$  corresponds to an axial rotation, one  $E''$  to two equatorial rotations, one  $A''_2$  to an axial translation and one  $E'$  to two equatorial translations. After eliminating these three translations and rotations

we are left with three even irreducible representations  $E'$ , as well as two  $A_2''$  and one  $E''$  odd representations. The six even normal modes ( $Q_1, \dots, Q_6$ ) transform in pairs like the partners of  $E'$ ; they have been obtained employing standard techniques [30,31] and are defined in table XI. In the same way the two modes  $A_2''$  ( $Q_7, Q_8$ ) and the two partners of  $E''$  ( $Q_9, Q_{10}$ ) have been obtained, and are defined in the same table.

The modes  $Q_3, Q_4$ , and  $Q_8$  are translations of only the two axial oxigens, and the  $Q_5, Q_6$ , and  $Q_7$  are translations of only the three equatorial oxigens while  $Q_9$  and  $Q_{10}$  are rotations along the  $x$  and  $y$  axis of the two axial oxigens. As these modes are only partial rotations or translations they are capable of changing the crystal field. The  $x$  and  $y$  rotations of the three equatorial oxigens can be combined with  $Q_9$  and  $Q_{10}$  to give full rotations of the trigonal bipyramid, and the  $z$  rotation of the three equatorial oxigens is already a full rotation, so these three sets of displacements would not appear in our calculation.

From tables VII, VIII, and IX we can calculate the displacements  $\mathbf{u}_j$  of the five O with respect to their positions in the reference trigonal bipyramid (cf. section III B 1) and calculate the corresponding normal modes  $Q_j$  defined in table XI. Employing these  $Q_j$  we calculate in the next two sections the  $g$  values of the distorted complex.

#### 4. The effect of the normal modes on the crystal field

We can now try and find an expression similar to Eq. (2) for the trigonal bipyramid. To this purpose we have employed a relation equivalent to Eq. (5) to calculate, for each of the ten normal modes  $Q_j$  given in table XI, the change in the crystal field  $V_{cf}(\mathbf{r})$  when all the ligands are displaced from their equilibrium position in the reference complex by a small fraction  $\varepsilon$  of that particular normal mode  $Q_j$ . Expanding this change of  $V_{cf}(\mathbf{r})$  in a power series of the coefficient  $\varepsilon$  and taking the linear terms in  $\varepsilon$  gives the corresponding  $V_j(\mathbf{r})$  from Eq. (2). As we are only interested in the subspace  $\{^4F, ^4P\}$  with  $S = 3/2$  of the configuration  $d^7$ , and the  $V_j(\mathbf{r})$  are independent of the spin component  $M_S$ , we need a 10x10 matrix  $\langle ^4L, M_S, M_L | V'_{CF} | ^4L', M_S, M'_L \rangle$  for each  $Q_j$ , with fixed  $M_S$  and  $L, L' = 3, 1$ . There are regularities between the matrix elements associated to different  $Q_j$ , and we shall employ the following abbreviations:  $Q_a = (Q_2 + iQ_1) + 5(Q_6 + iQ_5)$ ,  $Q_b = 3(Q_2 + iQ_1) + 7(Q_6 + iQ_5)$ ,  $Q_c = 9(Q_2 + iQ_1) + (Q_6 + iQ_5)$ ,  $Q_d = iQ_7$ , and  $Q_e = 9(Q_{10} + iQ_9)$ , as well as their complex conjugates  $Q_a^*$ ,  $Q_b^*$ ,  $Q_c^*$ ,  $Q_d^*$  and  $Q_e^*$ . In tables XII and XIII we give the non-zero matrix elements in the upper triangle of the submatrices  $^4F \times ^4F$  and  $^4P \times ^4P$  respectively, and in table XIV we give all those associated with  $^4P \times ^4F$ ; the remaining non-zero elements are obtained by Hermitian conjugation. It is interesting to note that the matrix elements associated to  $Q_3, Q_4$ , and  $Q_8$  are all zero: these modes involve only the two axial ions, and the corresponding two atom partial complex is not only invariant against the operations of  $D_{3h}$ , but also against a twofold axis along the  $z$  direction. This extra symmetry forces all the one-electron matrix elements between  $d$  states of the crystal field associated to  $Q_3, Q_4$ , and  $Q_8$  to be zero.

As in the crystal field of the reference complex, the  $V'_{CF}$  has coefficients containing the Co-O distances  $R_a$  and  $R_c$ , as well as the atomic averages  $\langle r^2 \rangle$  and  $\langle r^4 \rangle$ , and they appear as  $c_2$  and  $c_4$  in the tables XII, XIV and XIII. As the  $R_a$  and  $R_c$  are nearly the same, it is possible from Eq. (4) to relate the crystal field parameters  $D_s$  and  $D_t$  to these two

coefficients. Assuming that  $R_a = R_c$  we obtain  $c_2 = 14 D_s$  and  $c_4 = (168/25)D_t$ , but we have derived slightly better relations considering the difference between  $R_a$  and  $R_c$ :

$$\begin{aligned} c_2 &= \frac{7}{-(3/2) + 2 (R_a/R_c)^3} D_s, \\ c_4 &= \frac{21}{(9/8) + 2 (R_a/R_c)^5} D_t. \end{aligned} \quad (6)$$

As with the reference complex, we employ the 3-j coefficients to calculate the matrix elements of the crystal field  $V'_{CF}$  in the representation that diagonalizes the total  $J$  and  $J_z$ , because the doublets  $|d^7 \alpha SLJM_J\rangle$  are basis for the irreducible representations of the reference trigonal bipyramid, and the eigenstates of the reference complex would then belong to subspaces with fixed  $M_J$ . In section III B 2 we have shown that, with the two sets of parameters  $B$ ,  $D_s$  and  $D_t$  obtained in that section, the two lowest doublets belong to the  $M_J = 1/2$  and  $M_J = 3/2$  subspaces and that they are separated by more than  $75 \text{ cm}^{-1}$ , while the remaining doublets are more than  $2300 \text{ cm}^{-1}$  above them. A good approximation to calculate the effect of  $V'_{CF}$  on these levels is then to consider the total Hamiltonian inside the two subspaces  $M_J = 1/2, 3/2$ , and one has then to consider a matrix of  $26 \times 26$  elements, corresponding to values of  $J$  equal to  $9/2, \dots, 1/2$ . The eigenstates of this matrix show that there is no change in the relative position of the two lowest doublets, so that the ground state remains  $M_J = 1/2$ .

### 5. The $g$ -factors of the penta-coordinated $\text{Co}^{2+}$ .

To calculate the spin Hamiltonian we employ the traditional method [25]. In the present case we consider the four states of the two lowest doublets of the reference trigonal bipyramid calculated in section III B 2 as the eigenstates of the unperturbed Hamiltonian, with  $M_J = 1/2$  as the ground doublet and  $M_J = 3/2$  as the excited one. Both the Zeeman term and the crystal field  $V'_{CF}$  produced by the deformation of the normal modes are the perturbations, and in the usual way we find the gyromagnetic tensor  $\mathbf{g}$  in second order. We have calculated the three components of  $\mathbf{g}$  for the penta-coordinated  $\text{Co}^{2+}$  for all the sets of  $B$ ,  $D_s$  and  $D_t$  given in table X, and the results are given in table XV. The values corresponding to the reference trigonal bipyramid are given in the rows  $b_0$  and  $c_0$ , while those given in the rows  $b_j$  and  $c_j$  (with  $j = 1, 2$  for the phosphate and  $j = 1, 2, 3$  for the arsenate) have been calculated employing the normal modes  $Q_j$  derived from the crystallographic positions (cf. table VII) as discussed in section III B 3. One verifies in table XV that the average of the principal values of  $\mathbf{g}$  is not very different from 4.33, but that it changes with  $B$  and the crystal field parameters more than in the octahedral case. The rows  $b_1$  and  $c_1$  include the effect of all normal modes, while in  $b_2$  and  $c_2$  only the even modes are considered. In the phosphate case, the crystallographic  $Q_1 = Q_5 = 0$ , and for the arsenate we have also imposed this condition in rows  $b_3$  and  $c_3$ . From table XV we conclude that

- With only even modes and  $Q_1 = Q_5 = 0$  (compare rows  $b_2$  and  $c_2$  in phosphate and  $b_3$  and  $c_3$  in arsenate with rows  $b_1$  and  $c_1$ ) the average  $g$  is not altered by the lower symmetry crystal fields generated by the remaining normal modes, and these fields affect the equatorial components of  $\mathbf{g}$ , but leave their sum and the axial component unaffected.

- Only the axial  $g$ -factor is altered by the inclusion of the odd modes, while the two equatorial  $g$ -factors are not altered (compare rows  $b_1$  with  $b_2$  and  $c_1$  with  $c_2$ ). This result is true both with  $Q_1 = Q_5 = 0$  (in the phosphate) or otherwise (in the arsenate).
- The fields associated to the modes  $Q_1$  and  $Q_5$  change the sum of the two equatorial  $g$ -factors but leave the axial value unaffected (compare rows  $b_2$  with  $b_3$  and  $c_2$  with  $c_3$  in the arsenate).

From the calculations in the present section, it follows that one should observe an allowed ESR line of  $\text{Co}^{2+}$  from the penta-coordinated complex when that site is occupied. We have seen in Section II C that besides the lines associated to the octahedral spectra, there are some weak extra lines that could be interpreted as belonging to that complex: their estimated  $g$ -factors are given in rows b) of table III, and should be compared with the values given in table XV, that were calculated for different sets of parameters derived from the optical spectra and with normal modes calculated from the crystallographic positions. It is clear that the arsenate values in row  $c_3$  of table XV are fairly close to the estimated values in row  $b$  from table III. It is well known that the  $g(i)$  obtained from the crystallographically calculated normal modes are generally different from those experimentally observed, as discussed for the octahedral compounds (cf. section III A ), and we could expect that a good fitting could be obtained by making small changes in the crystallographic normal modes. To verify this assumption it is sufficient to change only  $Q_2$  and  $Q_6$ , keeping all the remaining modes at their crystallographic values. Employing  $Q_2/R_a = -0.03$  and  $Q_6/R_a = -0.07$  for the phosphate we find  $g(1) = 7.05$ ,  $g(2) = 3.03$ , and  $g(3) = 2.12$ , while for the arsenate we obtain  $g(1) = 7.62$ ,  $g(2) = 3.04$ , and  $g(3) = 1.99$  with  $Q_2/R_a = 0.01$  and  $Q_6/R_a = -0.07$ . These fittings are fairly good, and show that the ESR spectra of  $\text{Co}^{2+}$  in the two compounds can be described perfectly well within our theory, but the crystal fields obtained can not be taken too seriously because of the very large errors in the experimental  $\mathbf{g}$  tensor.

We notice that the relative intensities of the extra lines in Fig. 2 are rather smaller than those in Fig. 3. This can be understood because the concentration of  $\text{Co}^{2+}$  in the arsenate is ten times larger than in the phosphate, and this should also alter their relative occupations.

The rather small intensity of the lines that could be attributed to the penta-coordinated complex indicates a very small occupation of  $\text{Co}^{2+}$  in the penta-coordinated sites. To verify this conjecture, we present a molecular orbital calculation of the heat of formation of these compounds in the following section, and the results are compatible with the present conclusion.

### C. Molecular Orbital Calculations

The energetics of penta- and hexa-coordinated phosphate clusters has been assessed in terms of the molecular orbital theory. Heats of formation were calculated within the well known semi-empirical technique Parametric Model 3 (PM3) [32]. This is a technique derived from the Hartree-Fock approximation in combination with a minimal basis set expansion of the molecular orbitals. Here we used a special parametrization developed for transition metal atoms which is contained in the package SPARTAN [33]. Correlation and relativistic effects, which are not explicitly treated in this theory, are partly recovered from the adoption

of experimental data in the parametrization. Molecular geometries were obtained as follows: the central metal atom and the coordinates of the first neighboring five or six oxygen atoms were taken from the crystal structure of the compound  $\text{Co}_2(\text{OH})\text{PO}_4$ . The ligands were chosen to be phosphoric acid molecules,  $\text{OP}(\text{OH})_3$ , since they have all bonds saturated and are neutral. Geometry optimizations of the isolated ligand were carried out at the *ab-initio* 6-31G\*\* level of calculation, in which the atomic orbitals of the basis set are written as a linear combination of cartesian gaussian functions [34]. The proton-free oxygen atoms of the ligands were then placed in the crystallographic positions of the oxygens around the metal atom such that the O=P bond points to the M-O direction, as shown in Figs. 4 and 5. The PM3 heats of formation of the clusters  $[\text{M}(\text{OP}(\text{OH})_3)_n]^{2+}$ ,  $n = 5, 6$  and  $\text{M} = \text{Co}$  and  $\text{Zn}$  were calculated assuming that Zn ion just replace the Co ion at frozen ligands positions. This is a reasonable assumption since the pure Co and Zn crystals have very similar cell parameters. Co clusters are doublets so that the unrestricted (spin-polarized) PM3 Hamiltonian was adopted. Spin contamination was negligible in this calculation. In order to discount the energies associated to the ligands themselves, the heats of formation of the corresponding clusters without the central metal ion were computed. Results are shown in table XVI. The values in the first column are the contributions from the ligands to the metal clusters heats of formation. It is then possible to evaluate the relative stabilization of  $\text{Co}^{2+}$  and  $\text{Zn}^{2+}$  ions in the penta- and hexa-coordinated environments by making the difference between the values in columns two or three and column one. It gives the energies  $-1258.04$  kcal/mol and  $-1314.30$  kcal/mol, for  $\text{Co}^{2+}$  at the trigonal bipyramid and octahedral sites respectively, while for  $\text{Zn}^{2+}$  the values are  $346.19$  kcal/mol and  $340.00$  kcal/mol. These values show that Co prefers the octahedral site by an amount of  $\sim 56$  kcal, which is approximately 2.4 eV, and Zn is slightly more stable also at the octahedral site by  $\sim 6$  kcal, or 0.3 eV. This difference is due to the partially filled 3d orbitals of Co that interact with the lone pairs of the neighboring oxygens, giving a more covalent character to the interaction.

A more direct comparison was made through the calculation of the heat of formation of clusters where the metal atoms and first neighbors are in the conformation of the  $\text{Co}_2(\text{OH})\text{PO}_4$  unit cell, as illustrated in Fig 6. Two clusters were built such that in one the  $\text{Co}^{2+}$  ion occupies the hexa-coordinated site and  $\text{Zn}^{2+}$  ion is in the penta-coordinated site (cluster 1), while in the other (cluster 2)  $\text{Co}^{2+}$  and  $\text{Zn}^{2+}$  ions are exchanged. The phosphate ions in contact with both metal ions were substituted by  $\text{H}_2\text{PO}_4$  species and the remainder of the ligands were phosphoric acid molecules. The composition of these clusters is then  $[\text{CoZn}(\text{OH})(\text{H}_2\text{PO}_4)_2(\text{OP}(\text{OH})_3)_5]^{4+}$ . PM3 calculations gave  $\Delta H_f$  (cluster 1) =  $-2147.10$  kcal/mol and  $\Delta H_f$  (cluster 2) =  $-2094.44$  kcal/mol, that is, the cluster with  $\text{Co}^{2+}$  ion in the octahedral site is  $\sim 53$  kcal more stable than the other one. It is thus expected that Co impurities in the zinc compounds occupy preferentially the octahedral sites, and this conclusion agrees with very low intensity of the ESR lines attributed to  $\text{Co}^{2+}$  in the penta-coordinated sites of the dilute compounds, as discussed in the previous section.

#### IV. DISCUSSION AND CONCLUSIONS

Four compounds of the adamite type:  $\text{Zn}_2(\text{OH})\text{PO}_4$ ,  $\text{Mg}_2(\text{OH})\text{AsO}_4$ ,  $\text{Co}_2(\text{OH})\text{PO}_4$ , and  $\text{Co}_2(\text{OH})\text{AsO}_4$  have been synthesized and studied, and the measurement of the optical properties of the pure Co compounds and of the ESR of impurities of  $\text{Co}^{2+}$  in  $\text{Zn}_2(\text{OH})\text{PO}_4$  and

$\text{Mg}_2(\text{OH})\text{AsO}_4$  have been discussed. Crystal field theory has been employed to try and understand the experimental ESR results for the two  $\text{Co}^{2+}$  complexes with coordination five and six that are present in the adamite structure. The Racah parameter  $B$  as well as the crystal fields  $D_q$  for the octahedral complex and both  $D_s$  and  $D_t$  for the trigonal bipyramid one have been estimated from the assignments that were made of the diffuse reflectance spectrum of these two complexes. Two alternative sets of parameters were proposed for the penta-coordinated complex.

From the crystallographic structure, a reference octahedron centered in the  $\text{Co}^{2+}$  was defined, such that the normal modes of the complex corresponding to rotations and expansions would be zero and the remaining normal modes would not have any contribution of these irrelevant deformations. Using a method already applied [10] to study the ESR of  $\text{Co}^{2+}$  in  $\text{NH}_4\text{NiPO}_4 \cdot 6\text{H}_2\text{O}$ , the crystal fields that would reproduce the experimental  $\mathbf{g}$  tensor of the octahedral complex in both  $\text{Zn}_2(\text{OH})\text{PO}_4$  and  $\text{Mg}_2(\text{OH})\text{AsO}_4$  have been obtained.

As the penta-coordinated complex seems to have at most minor contributions to the ESR spectra, we have analyzed the possible motives for this behavior. We argue that two doublets with  $M_J = \pm 1/2$  and  $M_J = \pm 3/2$  would be lowest in energy, separated by a rather large excitation energy from the remaining excited states. The  $M_J = \pm 3/2$  has forbidden ESR transitions, and this would explain the experimental results if that were the ground doublet, but when the crystal field of the trigonal bipyramid is considered together with the spin-orbit interaction, it was found that the  $M_J = \pm 1/2$  doublet, with allowed ESR transitions, is the lowest. To verify whether this result would be altered by the deformations of the trigonal bipyramid, we considered their effects in a way similar to that employed in the octahedral case to calculate the  $\mathbf{g}$  tensor. First it was necessary to derive the normal modes of the trigonal bipyramid that are relevant to our problem, and they are given in table XI. The corresponding Jahn-Teller contributions  $V'_{CF}$  to the crystal field, whose non-zero matrix elements  $\langle {}^4L, M_S, M_L | V'_{CF} | {}^4L', M_S, M'_L \rangle$ , for  $L, L' = 3, 1$ , are given in tables XII, XIV and XIII. Defining a reference perfect trigonal bipyramid by the same method employed in the octahedral case, the values of the relevant normal modes were obtained by employing the crystallographic positions, and subsequently used to calculate their effect on the relative position of the two lowest doublets. No appreciable change was found, and as an alternative explanation we assumed that the penta-coordinated complex is scarcely occupied in the dilute system. To verify this conclusion, the heat of formation of the octahedral and the trigonal bipyramid complexes with both Co and Zn as the central ions were calculated, and it was found that their values are compatible with a rather small occupation of the penta-coordinated site.

Employing the Jahn-Teller crystal fields together with the normal modes calculated from the crystallographic distortions, it was possible to calculate the  $\mathbf{g}$  tensor, shown in table XV for both the perfect and deformed trigonal bipyramid, this last subjected to different deformations. The trace of the  $\mathbf{g}$  tensor in the perfect trigonal bipyramid changes more with the parameters  $B, D_s$  and  $D_t$  than in the octahedral case, where it is always fairly close to 13.

The trigonal bipyramid has no center of symmetry, and it was necessary to consider all the normal modes, even those that are odd against reflection in the horizontal symmetry plane. We have shown that these last modes affect the axial component of  $\mathbf{g}$  but that they have little or no effect on the two equatorial components. The experimental  $g$ -tensor

of the penta-coordinated complex could be measured but with rather large errors. As in the octahedral case, the crystallographically determined normal modes could not explain the observed values, but for the two type of complexes it was possible to find values of the normal modes that would generate crystal fields that describe the experimental ESR spectra for both the phosphate and arsenate compounds.

We conclude that both our theoretical analysis of the ESR of the systems studied, as well as the molecular orbital calculation of the formation energies. coincide in assigning a rather small relative occupation of the penta-coordinated sites with respect to the octahedral ones in those systems. We could also understand the experimental spectra of both the octahedral and penta-coordinated complexes by considering the effect of the crystal fields generated by the corresponding normal modes on the  $\mathbf{g}$  tensor.

### **ACKNOWLEDGMENTS**

The three first authors(MEF,MCS,GEB) would like to acknowledge financial support from the following agencies: FAPESP and CNPq .

## REFERENCES

- [1] H. Riffel, F. Zettler and H. Hess. *Neus Jahrb. Mineral. Monatsch.* 514 (1975).
- [2] W. E Richmond, *Am. Mineral.*, **25**, 441 (1940).
- [3] F. C. Hawthorne, *Can. Mineral.* **14**, 143 (1976).
- [4] R. J. Hill, *Am. Mineral.*, **61**, 979 (1976).
- [5] W.T.A., Harrison, J.T. Vaughey, L.L., Dussack, A.J., Jacobson, T.E. Martin and G.D. Stucky, *J. Solid State Chem.* **114** 151 (1995).
- [6] P. Keller *Neues. Jahrb. Mineral. Monatsh*, 560 (1971)
- [7] P. Keller, H. Hess and F. Zettler, *Neues Jahrb. Miner. Abh.*, **134**, 147 (1979).
- [8] J. M. Rojo, Ph. D thesis, Universidad del Pais Vasco, Bilbao, 2000
- [9] A. Abragam and B. Bleaney, *Electron Paramagnetic Resonance of Transition Ions* (Clarendon Press, Oxford, 1970). See pag. 449.
- [10] A. Goñi, L. M. Lezama, T. Rojo., M. E. Foglio, J. A. Valdivia and G. E. Barberis, *Phys. Rev. B* **57** 246 (1998).
- [11] F. G. Beltran and F. Palacio, *J. Phys. Chem.* **80** 1373 (1976).
- [12] F. Palacio, *J. Phys. Chem.* **82** 825 (1978).
- [13] H. A. Jahn and E. Teller, *Proc. Roy. Soc.(London) A*, **161** 220 (1937).
- [14] H. A. Jahn, *Proc. Roy. Soc.(London) A*, **164** 117 (1937).
- [15] J. M. Rojo, J. L. Mesa, L. Lezama, G. E. Barberis and T. Rojo, *J. Magn. Magn. Mat.* **157/158** 493 (1996).
- [16] T. Rojo, L. Lezama, J.M. Rojo, M. Insausti, M.I. Arriortua and G. Villeneuve, *Eur. J. Solid State Inorg. Chem.* **29** 217 (1992).
- [17] M. M. Rojo, J. L. Mesa, J. L Pizarro, L. Lezama, M. I Arriortua and T Rojo, *J. Solid State Chem.* **132** 107 (1997).
- [18] When we derive the system parameters of the octahedral complexes from the optical spectra, we have shifted the ground orbital level by the spin orbit correction, estimated to be  $2.5 \alpha\lambda \sim -635 \text{ cm}^{-1}$ . This improvement was not used in the penta-coordinated complex.
- [19] J. H. Van Vleck, *J. Chem. Phys.* **7** **72** (1939).
- [20] G. F. Koster, J. O. Dimmock, R. G. Wheeler and H. Stats, *Properties of the thirty-two point groups* (M.I.T.Press, Cambridge, Massachusetts, 1963).
- [21] M. Tinkham, *Proc. Roy. Soc.(London) A*, **236** 549 (1956).
- [22] L. T. Peixoto and M. E. Foglio, *Revista Brasileira de Física* **13** 564 (1983).
- [23] E. B. Tucker, *Phys. Rev.* **143** 264 (1966).
- [24] A. Abragam and M. H. L. Pryce, *Proc. Roy. Soc.(London) A*, **206** 173 (1951).
- [25] H. M. L. Pryce, *Proc. Roy. Soc.(London) A*, **63** 25 (1950).
- [26] J. S. Wood, *Inorg. Chem.* **7** 852 (1968).
- [27] J. S. Griffith, *The theory of transition-metal ions.* (University Press, Cambridge, England, 1961), see Eq. (6.37).
- [28] U. Fano and G. Racah, *Irreducible tensorial sets.*(Academic Press, New York, 1959).
- [29] C. W. Nielsen and G. F. Koster, *Spectroscopic coefficients for the  $p^n$ ,  $d^n$ , and  $f^n$  configurations.* (MIT Press, Boston, Mass. 1963).
- [30] L. A. Woodward, *Introduction to the theory of molecular vibrations and vibration spectroscopy.* (Clarendon Press, Oxford, 1972).

- [31] E. B. Wilson, J. C. Decius and P. C. Cross, *Molecular vibrations*. (McGraw-Hill, New York, 1955).
- [32] J.J.P. Stewart, *J. Comput. Chem* **10**, 209 (1989).
- [33] SPARTAN package v. 5 (Wavefunction Inc., 1995).
- [34] For basis set definitions, see for instance A. Szabo e N.S. Ostlund, *Modern Quantum Chemistry* (McGraw-Hill, New York, 1989).

TABLES

${}^4T_{1g} \rightarrow$	${}^4T_{2g}$	${}^4A_{2g}$	${}^4T_{1g}(P)$	<b>B</b>	<b>D<sub>q</sub></b>
PO <sub>4</sub>					
a)	8450	15450	18350		
b)	7819	16013	18324	767.6	819.4
AsO <sub>4</sub>					
a)	7700	15500	18020		
b)	7616	15585	18011	758.9	796.9

TABLE I. a) The transitions between the ground  ${}^4T_{1g}$  level and the levels shown at the top of each column, in  $\text{cm}^{-1}$  and assigned from the experimental spectra of the octahedral complexes of  $\text{Co}_2(\text{OH})\text{PO}_4$  and  $\text{Co}_2(\text{OH})\text{AsO}_4$ ; the level  ${}^4T_{1g}(P)$  corresponds to the highest of the same symmetry. b) The best fit, obtained with the  $B$  and  $D_q$  shown in the last two columns.

${}^4A'_2 \rightarrow$	${}^4A'_1, {}^4A'_2$	${}^4E''$	${}^4E'$	${}^4A'_2(P)$	${}^4E''(P)$
PO <sub>4</sub>					
a)	6400	7000	11100	15800	19600
b)	3233	4835	12868	17386	17947
c)	1511	3603	11106	15801	19604
AsO <sub>4</sub>					
a)	5000	6250	10870	16000	19800
b)	2707	4440	12210	17188	18595
c)	1437	3535	10876	15999	19805

TABLE II. a) The transitions between the ground level  ${}^4A'_1$  and the levels shown at the top of each column, given in  $\text{cm}^{-1}$  and assigned from the experimental spectra of the penta-coordinated complexes of  $\text{Co}_2(\text{OH})\text{PO}_4$  and  $\text{Co}_2(\text{OH})\text{AsO}_4$ . b) The best possible fit to the five transitions. c) The best fit obtained by adjusting only the three transitions of higher energy. The corresponding values of  $B$ ,  $D_s$ ,  $D_t$  are given in rows b) and c) of table X.

	$g_1$	$g_2$	$g_3$	$A_1$	$A_2$	$A_3$
PO <sub>4</sub>						
a	$5.89 \pm 0.02$	$4.55 \pm 0.05$	$2.02 \pm 0.02$	$240 \pm 5$	$155 \pm 8$	$85 \pm 3$
b	$8. \pm 0.5$	$3.2 \pm 0.3$	$2.0 \pm 0.2$			
AsO <sub>4</sub>						
a	$6.22 \pm 0.02$	$4.21 \pm 0.05$	$2.05 \pm 0.02$	$140 \pm 5$	$120 \pm 7$	$55 \pm 5$
b	$9. \pm 1.5$	$3. \pm 0.5$	$2.0 \pm 0.2$			

TABLE III. Values of the principal  $g$  and  $A$  parameters, obtained from the spectra in Figs. 2 and 3. The values of the  $A$  parameters are in  $10^{-4} \text{ cm}^{-1}$  units. a) Octahedral complex: the  $g$  and  $A$  values were obtained from a program simulating powder spectra, as described in the text. b) The parameters for the penta-coordinated  $\text{Co}^{2+}$ , also estimated by simulation.

<b>n</b>	<b>a</b> (Å)	<b>b</b> (Å)	<b>c</b> (Å)	<b>a</b> (Å)	<b>b</b> (Å)	<b>c</b> (Å)
	PO <sub>4</sub>			AsO <sub>4</sub>		
1	4.7150	-1.2420	0.0000	0.9197	-1.0794	0.0000
2	4.9627	-1.0327	2.9700	0.6438	-1.2633	3.0255
3	2.1592	-1.2713	1.7274	-1.9091	-1.1662	1.3476
4	3.0793	1.0327	2.9700	-0.6438	1.2633	3.0255
5	3.3270	1.2420	0.0000	-0.9197	1.0794	0.0000
6	5.8827	1.2713	1.7274	1.9091	1.1662	1.3476
7	4.0210	0.0000	1.5135	0.0000	0.0000	1.4910

TABLE IV. The columns **a,b,c** give the position of the six oxygens (n=1,...,6) and Cobalt (n=7) in the hexa-coordinated complexes of Co<sub>2</sub>(OH)PO<sub>4</sub> and Co<sub>2</sub>(OH)AsO<sub>4</sub> with respect to the three unit cell axes. The X,Y,Z axes roughly correspond to n=1,2,3 respectively, taking n=7 as the origin.

	<b>Q<sub>2</sub>/R</b>	<b>Q<sub>3</sub>/R</b>	<b>Q<sub>4</sub>/R</b>	<b>Q<sub>5</sub>/R</b>	<b>Q<sub>6</sub>/R</b>
	PO <sub>4</sub>				
a)	0	-0.04407	0.03478	0.03478	0.11425
b)	0	-0.11683	-0.01717	-0.01717	-0.05641
	AsO <sub>4</sub>				
a)	0	-0.0441	0.04032	0.04032	0.09989
b)	0	-0.09328	-0.02818	-0.02818	-0.06982

TABLE V. Normal modes of the octahedral Co divided by the Co-O distance R in Co:Zn<sub>2</sub>(OH)PO<sub>4</sub> and Co:Mg<sub>2</sub>(OH)AsO<sub>4</sub>. a) Values that adjust the experimental values of the g tensor. b) Values obtained from the crystallographic positions corresponding to the pure compounds.

	<b>X</b>	<b>Y</b>	<b>Z</b>	<b>X</b>	<b>Y</b>	<b>Z</b>
	PO <sub>4</sub>			AsO <sub>4</sub>		
<b>a</b>	0.4054	-0.5794	-0.7071	0.3800	-0.5963	-0.7071
<b>b</b>	0.4054	-0.5794	0.7071	0.3800	-0.5963	0.7071
<b>c</b>	-0.8194	-0.5733	0.0000	-0.8434	-0.5373	0.0000

TABLE VI. Direction cosines of the three axis **X,Y,Z** of the reference perfect octahedron of Co<sub>2</sub>(OH)PO<sub>4</sub> and Co<sub>2</sub>(OH)AsO<sub>4</sub> with respect to the three crystallographic axis **a, b, c**

<b>n</b>	<b>a</b> (Å)	<b>b</b> (Å)	<b>c</b> (Å)	<b>a</b> (Å)	<b>b</b> (Å)	<b>c</b> (Å)	
		PO <sub>4</sub>			AsO <sub>4</sub>		
1	4.9008	3.2438	2.9700	4.9744	0.9132	3.0180	
2	1.8617	2.9132	1.2426	1.9003	1.1604	1.3442	
3	1.8617	2.9132	4.6974	1.9003	1.1604	4.6676	
4	3.1412	5.1252	2.9700	3.2085	3.2015	3.0180	
5	3.0793	1.0327	2.9700	3.2736	-0.9132	3.0180	
6	2.9102	3.0621	2.9700	3.0056	1.1561	3.0180	

TABLE VII. The columns **a,b,c** give the position of the five oxygens (n=1,...,5) and Cobalt (n=6) in the penta-coordinated complexes of Co<sub>2</sub>(OH)PO<sub>4</sub> and Co<sub>2</sub>(OH)AsO<sub>4</sub> with respect to the three unit cell axes.

	<b>X</b>	<b>Y</b>	<b>Z</b>	<b>X</b>	<b>Y</b>	<b>Z</b>	
		PO <sub>4</sub>			AsO <sub>4</sub>		
<b>a</b>	0.	0.	1.	-0.00203	0.	0.999998	
<b>b</b>	0.99931	0.03720	0.	0.999698	-0.02449	0.00203	
<b>c</b>	-0.03720	0.99931	0.	0.02449	0.9997	0.00005	

TABLE VIII. Direction cosines of the three axis **X,Y,Z** employed to define the reference perfect trigonal bipyramid of Co<sub>2</sub>(OH)PO<sub>4</sub> and Co<sub>2</sub>(OH)AsO<sub>4</sub> with respect to the three crystallographic axis **a, b, c**

<b>n</b>	X	Y	Z
1	0	R <sub>a</sub>	0
2	$-\frac{\sqrt{3}}{2}R_a$	$-\frac{1}{2}R_a$	0
3	$\frac{\sqrt{3}}{2}R_a$	$\frac{1}{2}R_a$	0
4	0	0	R <sub>c</sub>
5	0	0	-R <sub>c</sub>
6	0	0	0

TABLE IX. The columns X,Y,Z give the position of the five oxygens (n=1,...,5) and Cobalt (n=6) in the reference perfect penta-coordinated complexes of Co<sub>2</sub>(OH)PO<sub>4</sub> [ $R_a = 2.01622$  Å and  $R_c = 2.04365$  Å], and Co<sub>2</sub>(OH)AsO<sub>4</sub> [ $R_a = 1.98578$  Å and  $R_c = 2.05596$  Å] with respect to the axes defined in table VIII

	<b>B</b>	<b>D<sub>s</sub></b>	<b>D<sub>t</sub></b>	<b>B</b>	<b>D<sub>s</sub></b>	<b>D<sub>t</sub></b>
	PO <sub>4</sub>			AsO <sub>4</sub>		
<b>b</b>	728.	165.	947.	785.	313	919.
<b>c</b>	852.	745.	885.	875.	749.	869.

TABLE X. The values of  $B$ ,  $D_s$ ,  $D_t$  in  $\text{cm}^{-1}$  that fit the optical transitions, given in table II, of the two penta-coordinated complexes. The best fit to the five transitions is given in row b), and the best fit to the three highest transitions in row c). The spin orbit parameter  $\zeta = 580 \text{ cm}^{-1}$  was used in all these fittings

$Q_j$	$x_1$	$y_1$	$z_1$	$x_2$	$y_2$	$z_2$	$x_3$	$y_3$	$z_3$	$x_4$	$y_4$	$z_4$	$x_5$	$y_5$	$z_5$
$2\sqrt{3}Q_1$	-2	0	0	1	$\sqrt{3}$	0	1	$-\sqrt{3}$	0	0	0	0	0	0	0
$2\sqrt{3}Q_2$	0	2	0	$\sqrt{3}$	-1	0	$-\sqrt{3}$	-1	0	0	0	0	0	0	0
$\sqrt{2}Q_3$	0	0	0	0	0	0	0	0	0	1	0	0	1	0	0
$\sqrt{2}Q_4$	0	0	0	0	0	0	0	0	0	0	1	0	0	1	0
$\sqrt{3}Q_5$	1	0	0	1	0	0	1	0	0	0	0	0	0	0	0
$\sqrt{3}Q_6$	0	1	0	0	1	0	0	1	0	0	0	0	0	0	0
$\sqrt{3}Q_7$	0	0	1	0	0	1	0	0	1	0	0	0	0	0	0
$\sqrt{2}Q_8$	0	0	0	0	0	0	0	0	0	0	0	1	0	0	1
$\sqrt{2}Q_9$	0	0	0	0	0	0	0	0	0	0	-1	0	0	1	0
$\sqrt{2}Q_{10}$	0	0	0	0	0	0	0	0	0	1	0	0	-1	0	0

TABLE XI. The six even (1-6) and four odd (7-10) normal modes  $E'$  that are relevant to our problem. The numbers are the coefficients of the departures  $\mathbf{u}_j = \{x_j, y_j, z_j\}$  of the  $j$ -th ion from their equilibrium position.

$M_L$	$M'_L$	$\langle {}^4F, M_S, M_L   V'_{CF}   {}^4F, M_S, M'_L \rangle$
-3	-2	$-(3 c_2 + 10 c_4) Q_e^* / (7\sqrt{3})$
-3	-1	$(6 c_2 Q_a - 15 c_4 Q_b) / (56\sqrt{5})$
-3	0	$\sqrt{15} c_4 Q_d / 4$
-3	1	$-\sqrt{5} c_4 Q_c^* / 16$
-2	-1	$-(9 c_2 - 40 c_4) Q_e^* / (21\sqrt{5})$
-2	0	$(12 c_2 Q_a + 5 c_4 Q_b) / (56\sqrt{10})$
-2	1	$\sqrt{5} c_4 Q_d / (2\sqrt{6})$
-2	2	$-5 c_4 Q_c^* / (16\sqrt{3})$
-1	0	$-\sqrt{2} (3 c_2 - 25 c_4) Q_e^* / (35\sqrt{3})$
-1	1	$(18 c_2 Q_a + 25 c_4 Q_b) / (140\sqrt{3})$
-1	2	$-\sqrt{5} c_4 Q_d / (2\sqrt{6})$
-1	3	$-\sqrt{5} c_4 Q_c^* / 16$
0	1	$\sqrt{2} (3 c_2 - 25 c_4) Q_e^* / (35\sqrt{3})$
0	2	$(12 c_2 Q_a + 5 c_4 Q_b) / (56\sqrt{10})$
0	3	$-\sqrt{15} c_4 Q_d / 4$
1	2	$(9 c_2 - 40 c_4) Q_e^* / (21\sqrt{5})$
1	3	$(6 c_2 Q_a - 15 c_4 Q_b) / (56\sqrt{5})$
2	3	$(3 c_2 + 10 c_4) Q_e^* / (7\sqrt{3})$

TABLE XII. The non-zero matrix elements of the crystal field  $V'_{CF} = \sum_j Q_j V_j(\mathbf{r})$  generated by the normal modes  $Q_1, \dots, Q_{10}$  between states  $|\alpha, S, M_S, L, M_L\rangle = |{}^4F M_S M_L\rangle$  in the subspace  ${}^4F \times {}^4F$ . Only the elements corresponding to the upper triangle of the matrix are given, and the remaining ones are obtained by Hermitian conjugation. The matrix is independent of, and diagonal in, the spin components  $M_S$ . To compress the table we have used the following abbreviations:  $Q_a = (Q_2 + iQ_1) + 5(Q_6 + iQ_5)$ ,  $Q_b = 3(Q_2 + iQ_1) + 7(Q_6 + iQ_5)$ ,  $Q_c = 9(Q_2 + iQ_1) + (Q_6 + iQ_5)$ , (even modes) and  $Q_d = iQ_7$ ,  $Q_e = (iQ_9 + Q_{10})$  (odd modes), as well as their complex conjugates  $Q_a^*$ ,  $Q_b^*$ ,  $Q_c^*$ ,  $Q_d^*$  and  $Q_e^*$ .

$M_L$	$M'_L$	$\langle {}^4P, M_S, M_L   V'_{CF}   {}^4P, M_S, M'_L \rangle$
-1	0	$3 c_2 Q_e^* / 5$
-1	1	$-3\sqrt{3} c_2 Q_a / 20$
0	1	$-3 c_2 Q_e^* / 5$

TABLE XIII. Same as in table XII but for the sub-matrix  ${}^4P \times {}^4P$ . The same abbreviations are used here.

$M_L$	$M'_L$	$\langle {}^4P, M_S, M_L   V'_{CF}   {}^4F, M_S, M'_L \rangle$
-1	-3	$(72 c2 Q_a^* - 5 c4 Q_b^*) / (56\sqrt{30})$
-1	-2	$\sqrt{2}(12 c2 + 5 c4) Q_e / (7\sqrt{15})$
-1	0	$-2(18 c2 + 25 c4) Q_e^* / 105$
-1	1	$(24 c2 Q_a - 25 c4 Q_b) / (280\sqrt{2})$
-1	2	$\sqrt{5} c4 Q_d / 4$
-1	3	$-\sqrt{5} c4 Q_c^* / (8\sqrt{6})$
0	-3	$-\sqrt{5} c4 Q_d / (4\sqrt{3})$
0	-2	$(12 c2 Q_a^* + 5 c4 Q_b^*) / (28\sqrt{10})$
0	-1	$\sqrt{2}(24 c2 - 25 c4) Q_e / (35\sqrt{3})$
0	1	$-\sqrt{2}(24 c2 - 25 c4) Q_e / (35\sqrt{3})$
0	2	$(12 c2 Q_a + 5 c4 Q_b) / (28\sqrt{10})$
0	3	$-\sqrt{5} c4 Q_d / (4\sqrt{3})$
1	-3	$-\sqrt{5} c4 Q_c / (8\sqrt{6})$
1	-2	$\sqrt{5} c4 Q_d / 4$
1	-1	$(24 c2 Q_a^* - 25 c4 Q_b^*) / (280\sqrt{2})$
1	0	$2(18 c2 + 25 c4) Q_e^* / 105$
1	2	$-\sqrt{2}(12 c2 + 5 c4) Q_e / (7\sqrt{15})$
1	3	$(72 c2 Q_a - 5 c4 Q_b) / (56\sqrt{30})$

TABLE XIV. Same as in table XII but for the sub-matrix  ${}^4P \times {}^4F$ . All the non zero matrix elements are given here, and those corresponding to the sub-matrix  ${}^4F \times {}^4P$  are obtained by Hermitian conjugation. The same abbreviations are used here.

	$g_1$	$g_2$	$g_3$	$g_{av}$
		PO <sub>4</sub>		
$b_0$	4.8027	4.8027	1.9904	3.8653
$b_1$	5.0477	4.5577	2.2998	3.9684
$b_2$	5.0477	4.5577	1.9904	3.8653
$c_0$	5.0435	5.0435	1.9829	4.0233
$c_1$	5.7379	4.3492	2.1171	4.0680
$c_2$	5.7379	4.3492	1.9829	4.0233
		AsO <sub>4</sub>		
$b_0$	4.8723	4.8723	1.9885	3.9110
$b_1$	5.7637	4.2279	2.2364	4.0760
$b_2$	5.7637	4.2279	1.9885	3.9934
$b_3$	5.6402	4.1044	1.9885	3.9110
$c_0$	5.0667	5.0667	1.9818	4.0384
$c_1$	7.1232	3.5385	1.9854	4.2157
$c_2$	7.1232	3.5385	1.9818	4.2145
$c_3$	6.8591	3.2744	1.9818	4.0384

TABLE XV. The principal components of the calculated  $\mathbf{g}$  tensor for the penta-coordinated Co<sup>2+</sup> and their average  $g_{av}$  in Co:Zn<sub>2</sub>(OH)PO<sub>4</sub> and Co:Mg<sub>2</sub>(OH)AsO<sub>4</sub>. The rows  $b_0$  and  $c_0$  are for the reference trigonal bipyramid, while  $b_1$ ,  $b_2$ ,  $b_3$ ,  $c_1$ ,  $c_2$ , and  $c_3$  include the effect of deformations produced by the crystallographically calculated normal modes. Rows  $b_1$  and  $c_1$  include all the normal modes, while  $b_2$  and  $c_2$  only include the even modes, and in rows  $b_3$  and  $c_e$  we have also put  $Q_1 = Q_2 = 0$ . The values of  $B$ ,  $D_s$ ,  $D_t$  and  $\zeta$  employed here for rows  $b_j$  ( $j = 0 - 3$ ) are given in row b of table X, and those corresponding to rows  $c_j$  are given in row c of that table.

$\Delta H_f$ (kcal/mol)	no ion	Co <sup>2+</sup>	Zn <sup>2+</sup>
$[\text{M}(\text{OP}(\text{OH})_3)_5]^{2+}$	-1214.69	-2472.73	-868.50
$[\text{M}(\text{OP}(\text{OH})_3)_6]^{2+}$	-1440.16	-2754.45	-1100.15

TABLE XVI. Heats of formation, in kcal/mol, from PM3 calculations.

## FIGURES

FIG. 1. Diffuse reflectance spectra for the a)  $\text{Co}_2(\text{OH})\text{PO}_4$  and b)  $\text{Co}_2(\text{OH})\text{AsO}_4$ . The horizontal scale is linear in the wavelength, but has been labeled employing the corresponding wavenumbers.

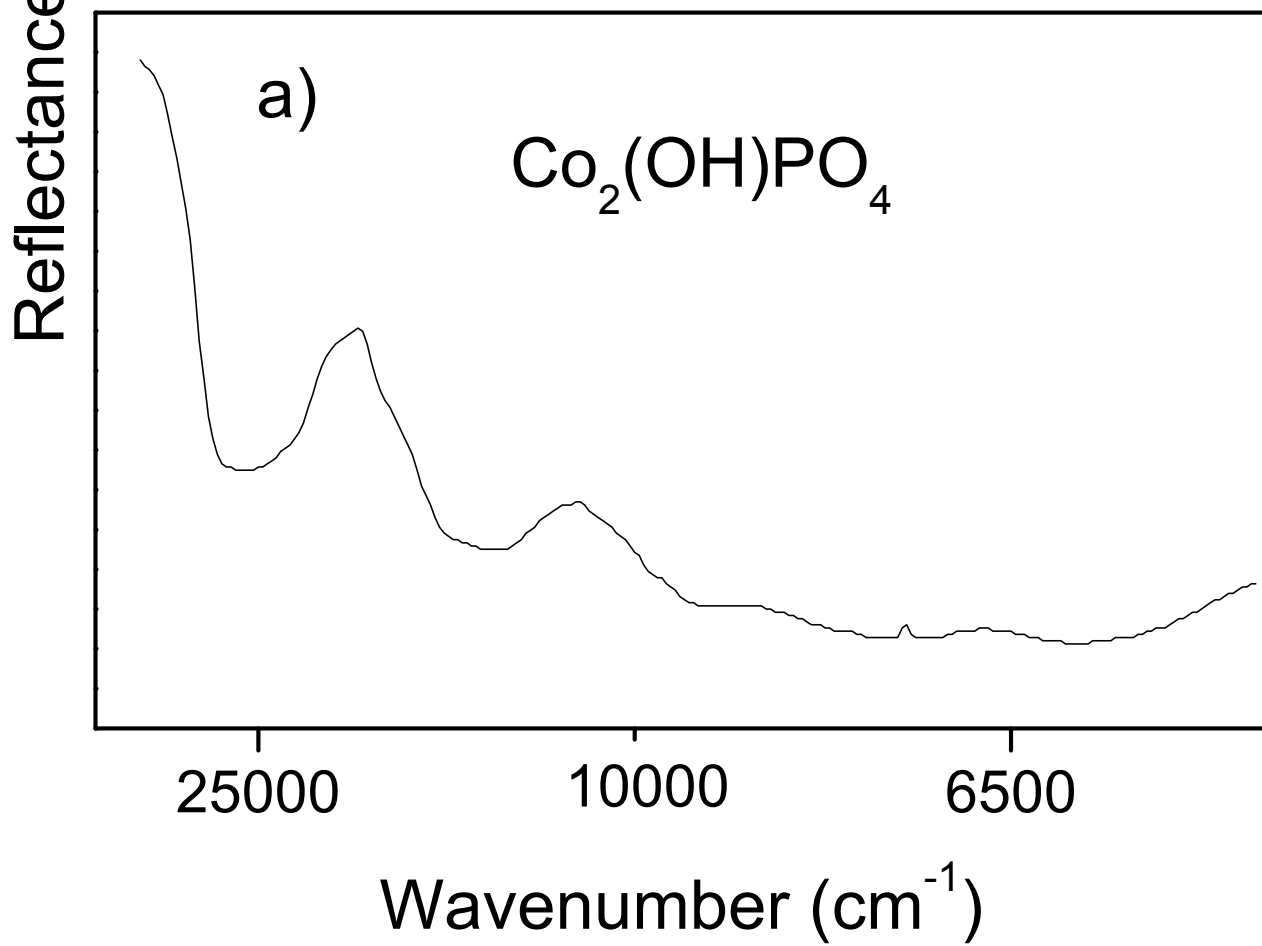
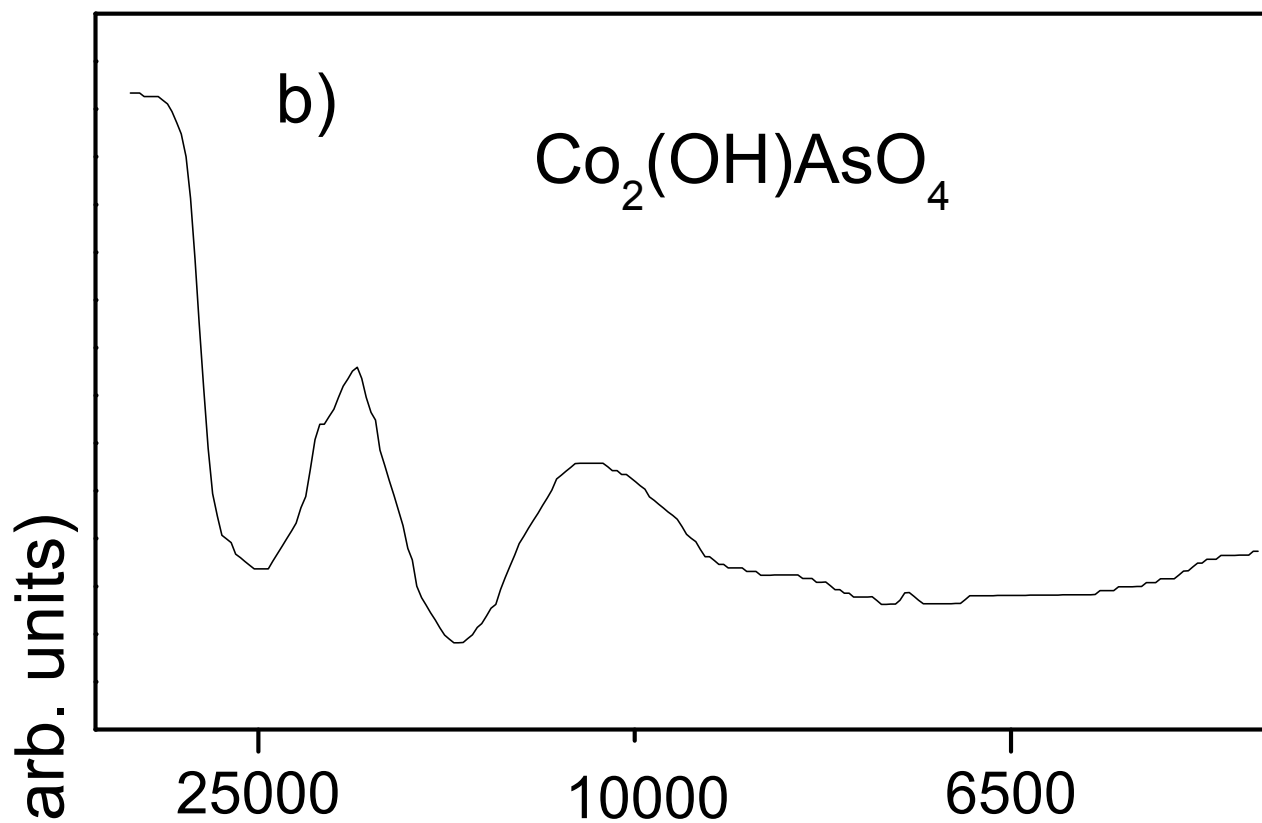
FIG. 2. ESR spectra of  $\text{Co}^{2+}$  in  $\text{Zn}_2(\text{OH})\text{PO}_4$ . a) Experimental spectrum. b) Sum of the simulated spectrum for both the hexa-coordinated and penta-coordinated complexes. c) Simulated spectrum for the hexa-coordinated complex. The g-values of both the octahedral and of the penta-coordinated complexes are given in table III. The arrows in c) show the g-values and their positions for the octahedral complex, while those in a) correspond to the penta-coordinated complex. The insert gives the detail of the experimental hyperfine structure and of the simulated one (around  $g_2$ ), attributed to the  $\text{Co}^{2+}$  in the triangular bipyramid.

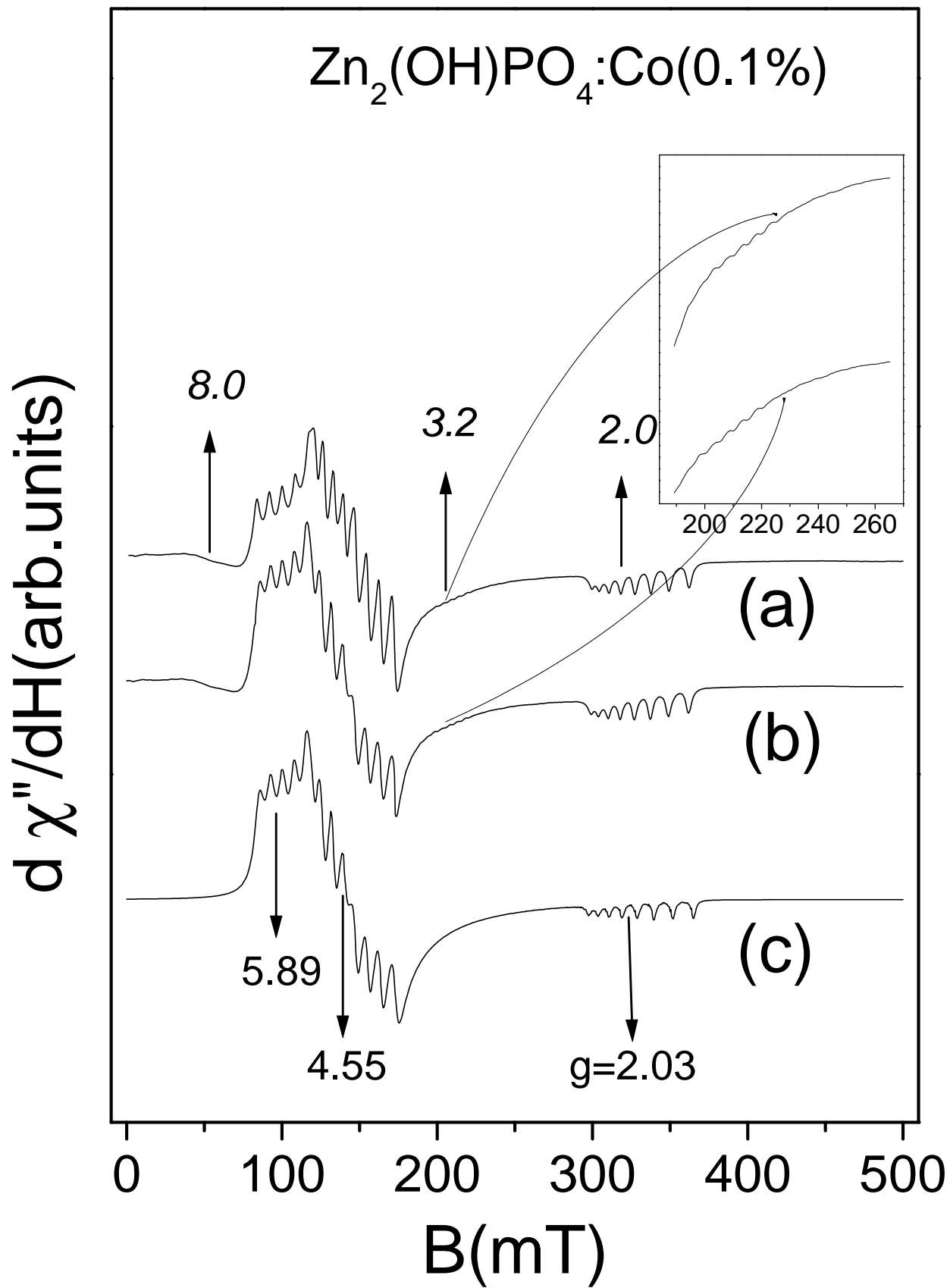
FIG. 3. ESR spectra of  $\text{Co}^{2+}$  in  $\text{Mg}_2(\text{OH})\text{AsO}_4$ . Curves a), b), and c), and the meaning of the arrows and values in curves a) and c) are the same as in figure 2.

FIG. 4. Ball-and-stick model of the penta-coordinated metal clusters with phosphoric acid molecules as ligands. One atom of each type is labeled in the figure.

FIG. 5. Hexa-coordinated metal/phosphoric acid cluster. One atom of each type is labeled in the figure.

FIG. 6. Cobalt/Zinc cluster built from the atomic coordinates of the  $\text{Co}_2(\text{OH})\text{PO}_4$  unit cell. Part of the phosphate ions were replaced by phosphoric acid molecules. One atom of each type is labeled in the figure, which shows the Co in the penta-coordinated position





$\text{Mg}_2(\text{OH})\text{AsO}_4:\text{Co}$  (1%)

